International Journal of Biological Macromolecules 101 (2017) 967–972

Contents lists available at ScienceDirect

International Journal of Biological Macromolecules

journal homepage: www.elsevier.com/locate/ijbiomac

Sodium alginate and gum acacia hydrogels of zinc oxide nanoparticles reduce hemolytic and oxidative stress inflicted by zinc oxide nanoparticles on mammalian cells

R. Raguvaran[a,b], Anju Manuja[a,*], Balvinder K. Manuja[a], T. Riyesh[a], Sandeep Singh[a], M. Kesavan[b], U. Dimri[b]

[a] ICAR-National Research Centre on Equines Sirsa Road, Hisar, Haryana, India
[b] Indian Veterinary Research Institute, Bareilly, UP, India

ARTICLE INFO

Article history:
Received 4 January 2017
Received in revised form 27 February 2017
Accepted 29 March 2017
Available online 31 March 2017

Keywords:
Zinc oxide nanoparticles
Reactive oxygen species
Oxidative stress
Alginate
Gum acacia
Horse
Lipid peroxidation
MDA
Hemolytic activity

ABSTRACT

Zinc oxide nanoparticles are important nanomaterials currently under research due to their applicability in nanomedicine. Toxicity of ZnO NPs has been extensively studied and has been shown to affect various cell types and animal systems. In this study, we investigated hemolytic potential and oxidative stress inflicted by ZnO NPs and ZnO NPs-loaded-sodium alginate-gum acacia hydrogels on horse erythrocytes and African green monkey kidney (Vero) cells. Our study provides a better understanding of the hemolytic and oxidative effects of interaction of ZnO NPs and ZnO NPs released from polymeric hydrogels with the biological system. Remarkable aggregation of erythrocytes was noted in the higher concentration of ZnO NPs treated erythrocytes as compared to erythrocytes treated with ZnO NPs-loaded hydrogels. ZnO NPs-loaded hydrogels treated Vero cells significantly reduced oxidative stress as evidenced by less malondialdehyde production as compared to that of ZnO NPs treated cells. Normal horse erythrocytes when treated with ZnO NPs in in vitro condition undergo oxidative damage, and contribute in augmenting the toxicity. We demonstrated that polymeric ZnO NPs reduced the undesirable effects provoked by ZnO NPs on mammalian cells.

1. Introduction

The rapidly developing nanotechnology has offered a plethora of novel nanoparticles for diverse applications [1–4]. Due to the extraordinary physiochemical properties, upon interaction with biological tissues and cells, some of the nano-scale materials pose an extraordinary hazard to animals and humans [5]. This property has attracted the attention of researchers for thorough toxicological evaluation of nanomaterials [5,6]. Metal oxide in the nano range acquires distinctive properties that primarily depend on size, chemical composition and surface chemistry. Metal oxide nanomaterials are most commonly used in sensors, catalysis, environmental sanative and personal care products [7,8]. Among the metal oxide nanoparticles, the zinc oxide nanoparticles (ZnO NPs) are most commonly used for antimicrobial properties [9]. The toxicity of each of these materials depends greatly upon the particular arrangement of its many atoms. Commonly the toxicity of NPs is associated with its small size and high surface area and therefore nanoforms are theoretically expected to be more toxic than their macro counterparts [10]. Metallic nanoparticles tend to disperse and release ions when exposed to a biological milieu resulting in reactive oxygen species (ROS) production and oxidative stress [11–14]. $Zinc^{2+}$ is an essential element in cell homoeostasis and remains in the bound form inside cells because free Zn^{2+} is very reactive and becomes cytotoxic [15]. The sudden increase of free Zn2+ levels may damage lysosomes allowing the contents to release into the cytoplasm and ultimately causing cell death [16,17].

Toxicity of ZnO NPs has been extensively studied and has been shown to affect various cell types and animal systems [18–23]. Previously we have shown that interaction of different concentrations of ZnO NPs with horse erythrocyte revealed concentration- dependent clustering of RBC [24]. The studies revealed evidence that the cytotoxicity of ZnO NPs may be partially due to their induction of cellular oxidative stress [25,26]. We developed ZnO hydrogels for the effective delivery of ZnO NPs using polymers sodium alginate/gum acacia (SAGA-ZnO NPs) to prevent undesirable effects [9,27]. Hence, in our study, we have investigated the oxidative

* Corresponding author at: ICAR-National Research Centre on Equines, Hisar 125001, Haryana, India.
E-mail address: amanuja@rediffmail.com (A. Manuja).

http://dx.doi.org/10.1016/j.ijbiomac.2017.03.180
0141-8130/

stress inflicted on Vero cells by the interaction of ZnO NPs, SAGA-ZnO NPs at varying concentrations. Further, we also evaluated the hemolytic potential of ZnO NPs/SAGA-ZnO NPs inflicted on horse erythrocytes.

2. Materials and methods

2.1. Synthesis of sodium alginate and gum acacia ZnO NPs

SAGA-ZnO NPs were synthesized using sodium alginate and gum acacia as described previously with some modifications [27]. Briefly, ZnO NPs were added to the aqueous solution of 1% w/v alginate sodium. After the addition of 0.1% w/v of an aqueous solution of gum acacia (GA), the crosslinker glutaraldehyde (1% of GA) was added dropwise under constant stirring. SAGA-ZnO NPs were pelleted out by centrifugation at 12000 rcf for 45 min at 4 °C. The blank hydrogels were prepared similarly but without the addition of ZnO NPs.

3. Morphology and particle size

Dynamic light scattering (DLS) was used to measure the average particle size and size distribution (polydispersity index) of formulated nanocapsules at 25 °C using the Zetasizer nano ZS (Malvern instruments, Malvern, UK).

The morphology of the SAGA-ZnO NPs was determined by transmission electron microscopy (TEM). The samples for TEM were prepared by placing a drop (20–25 μl) of the solution onto a 400 mesh copper grid coated with carbon. About 1 min after deposition, the grid was tapped with a filter paper to remove surface water and then examined under transmission electron microscope (JEOL 100) with high contrast imaging mode at an acceleration of 100 KV.

3.1. Cell culture

A mammalian Vero (African green monkey kidney) cell line was obtained from the Veterinary Type Culture Collection (VTCC), NRCE, Hisar and maintained in Eagle's minimum essential medium (EMEM) supplemented with HEPES 10 mM, L-glutamine 2 mM, sodium bicarbonate 25 mM and 1% antibiotics-antimycotic solution (penicillin 10000 units/ml, streptomycin–10 mg/ml, amphotericin B 25 μg/ml) at 37 °C in 5% carbon dioxide (CO_2).

3.2. Determination of lipid peroxidation induced by ZnO NPs and SAGA-ZnO NPs

Levels of malondialdehyde (MDA) were determined as thiobarbituric acid-reactive substances (TRABS) in the supernatants of cultures of the ZnO NPs, SAGA-ZnO NPs, blank hydrogel, treated and untreated Vero cell line as described previously [28]. Briefly, to 100 μl of supernatant, 80 μl of 15% trichloroacetic acid (TCA) and 160 μl of 0.67% thiobarbituric acid (TBA) were added and were vortexed. After incubation at 95 °C in a water bath for 20 min, 600 μl of butanol was added and mixed gently. The quantity of 200 μl of butanol phase was added to 96 well plate in designated wells and optical density (OD) of each well was measured at 535 nm in UV spectrophotometer (Biotek instruments, powerwave X2, USA). MDA concentration in the sample was calculated by using the molar absorption coefficient $\epsilon = 1.56 \times 0^5\ M^{-1}\ cm^{-1}$ in Beer- Lambert law as per the formula

$$A = \epsilon.c.l,$$

where, A – OD value of the sample, ϵ – Molar absorption coefficient, l – Path length of 96 well plate, c is MDA/hydroperoxide concentration.

3.3. Effect of ZnO NPs, SAGA-ZnO NPs on horse RBC

3.3.1. Hemolytic activity of ZnO NPs

We assessed the effect of ZnO NPs, SAGA-ZnO NPs, blank hydrogel, positive control (distilled water), solubilising buffer (negative control) on horse RBCs by hemolytic assay and phase contrast microscope [24,28,29]. The RBC pellets obtained from the blood of adult Marwari horses after centrifugation and subsequent washings with phosphate buffered saline (PBS, pH 7.2) was suspended in equal volume of PBS. The two-fold serial different concentrations from 10 mg/ ml to 0.625 mg/ml of test samples were prepared in solubilising buffer *i:e* PBS containing 10% dimethylformamide (DMF). The RBC suspension was added to the test samples in the ratio of 1:10 in designated wells of 96 well plate and incubated at 37 °C for 90 min followed by centrifuging at 3000 rpm for 5 min. The supernatants were transferred to new 96 well plate in the designated wells. The absorbance of the samples was measured at 543 nm using UV spectrophotometer (Biotek instruments, powerwave X2, USA). The percentage of hemolysis of ZnO NPs, SAGA-ZnO NPs, blank hydrogel along with positive and negative controls at a given concentration was calculated by following formula

$$H = \{(OD_S - OD_0)/(OD_{100} - OD_0)\} \times 100$$

Where H is the percentage of hemolysis; OD_S, OD_0, OD_{100} are optical densities of test, negative and positive samples respectively. To ascertain the hemolysis of RBC by phase contrast microscopy, RBC suspension was further diluted 20 times in solubilising buffer, treated with ZnO NPs, SAGA-ZnO NPs, blank hydrogel (final concentration: 2 mg/ml to 0.25 mg/ml) along with positive and negative controls and incubated at 37 °C for 3 h. Blood smears were then prepared and examined under phase contrast microscope.

3.4. Statistical analysis

All experiments were performed in triplicate, and the results were exhibited as a mean ± standard deviation. Statistical differences among groups were determined using the Student's *t*-test (two-tailed, equal variances) using online graphpad software (http://www.graphpad.com/quickcalcs/ttest1.cfm). The statistical significance was accepted at a level of $p < 0.05$.

4. Results and discussion

4.1. Characterization of ZnO NPs and SAGA-ZnO NPs

Particle size analysis was performed by photon correlation spectroscopy (PCS). The PCS yields the mean diameter (z-average) of the bulk population of the particles and additionally a polydispersity index (PdI) as a measure for the width of the distribution. The PdI ranges from 0 (monodisperse) to 0.500 (very broad distribution). The particle diameter (z-average) of SAGA-ZnO NPs were 180 nm. The representative figures showing particle size as 139.2 nm with PdI 0.265 for SAGA-ZnO NPs (Fig. 1A). The TEM micrographs show ovoid SAGA-ZnO NPs of approximate 58.95 nm (Fig. 1B)

4.2. Oxidative stress induced by ZnO NPs and SAGA-ZnO NPs

Oxidative stress was shown to be one of the predominant ways of nanoparticle toxicity and stress in various cell lines. Literature suggests numerous metallic elements are nephrotoxicants that preferentially accumulate and produce cellular injury in the

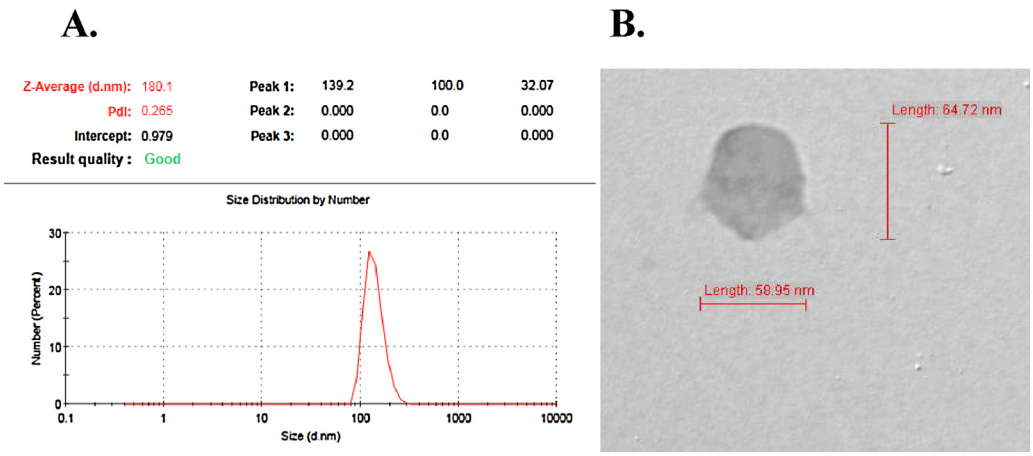

Fig. 1. A. Particle size analysis of SAGA-ZnO NPs showing polydispersity index. B. Images of in SAGA-ZnO NPs viewed under Transmissible electron microscope (TEM).

kidneys [30]. Human kidney cells have been used to assess the toxicity profile of ZnO NPs [30]. Kidney Vero Cell Line has been described as a suitable model to study the toxicity of microcystins [31]. We thought pertinent to evaluate SAGA-ZnO NPs and ZnO NPs on Vero cell line derived from African monkey kidney. Lipid peroxidation by TBA assay using SAGA-ZnO NPs and ZnO NPs showed concentration-dependent oxidative stress in our study. It was significantly higher in ZnO NPs treated cells at higher concentration compared to SAGA-ZnO NPs ($P < 0.001$). In lower concentrations also, it was significantly higher in ZnO NPs treated cells ($P < 0.05$). Malondialdehyde is a breakdown product of lipids which can be quantified as a measure of lipid hydroperoxides [28]. Oxidative stress based on malondialdehyde (MDA) production is shown in Fig. 2. The observation on concentration dependent oxidative stress corroborates with the findings of researchers performing on liver tissue homogenate, human neuronal cells and cardiac cells [32–34]. The results of our study demonstrate that ZnO NPs induce cytotoxicity in Vero cell line and this effect is likely to be mediated through ROS generation and oxidative stress. In SAGA-ZnO NPs treated Vero cells significantly reduced oxidative stress was noticed due to the sustained release mechanism of ZnO NPs.

4.3. Erythrocyte morphology and hemolytic assay

We assessed the hemolytic impact of ZnO NPs and SAGA-ZnO NPs on horse erythrocytes. The general morphology of the erythrocytes treated with ZnO NPs and SAGA-ZnO NPs by phase-contrast microscopy is shown in Fig. 3A. The suspension of RBC was treated with different concentrations of ZnO NPs, SAGA-ZnO NPs and blank hydrogel and subsequent spectrophotometric evaluation revealed none of the nanoformulations was toxic to RBC even at higher concentration. The hemolytic pattern of different concentration of ZnO NPs, SAGA-ZnO NPs and blank hydrogel along with positive and negative control are shown in Fig. 3B.

Hemolytic potential of ZnO NPs must be evaluated before their clinical application due to the possible occurrence of hemolytic jaundice and anemia. Hemolysis as an expression of nanoparticles induced cytotoxicity in red blood cell by spectrophotometer evaluation revealed none of the nanoformulations was toxic to RBC except the distilled water control in our study. TiO_2 nanoparticles after 24 h incubation with erythrocyte showed clustered RBC under a microscope [35]. Erythrocyte suspension treated with different concentrations of ZnO NPs and SAGA-ZnO NPs were analyzed under phase contrast microscope to detect any changes in the morphology. After 3 h incubation of RBC with different concentrations of

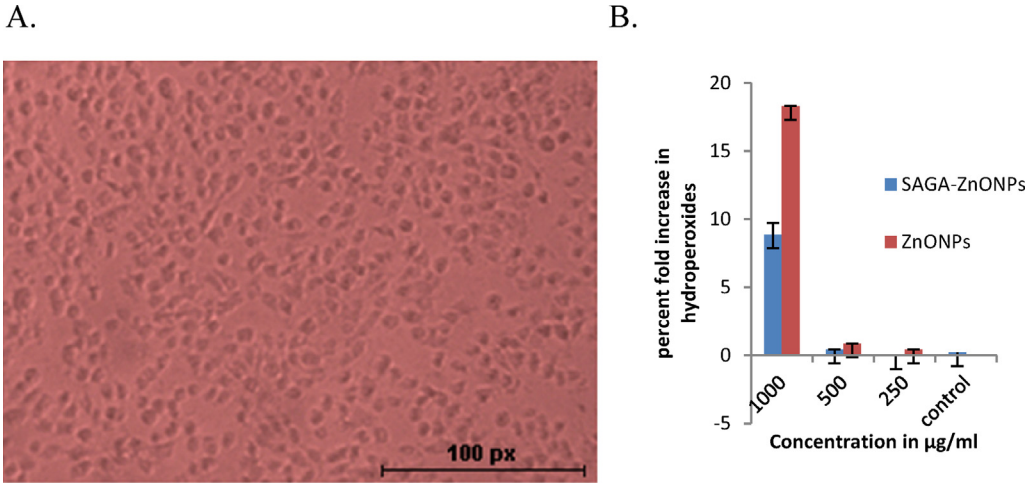

Fig. 2. A. Photomicrograph of Vero cells cultured in EMEM medium (400x) B. Hydroperoxide levels produced by Vero cells in response to different concentration of ZnO NPs and SAGA-ZnO NPs. Percent fold increase in hydroperoxide levels in response to different concentration of ZnO NPs and SAGA-ZnO NPs is expressed relative to untreated Vero cells. Error bars show the standard deviation.

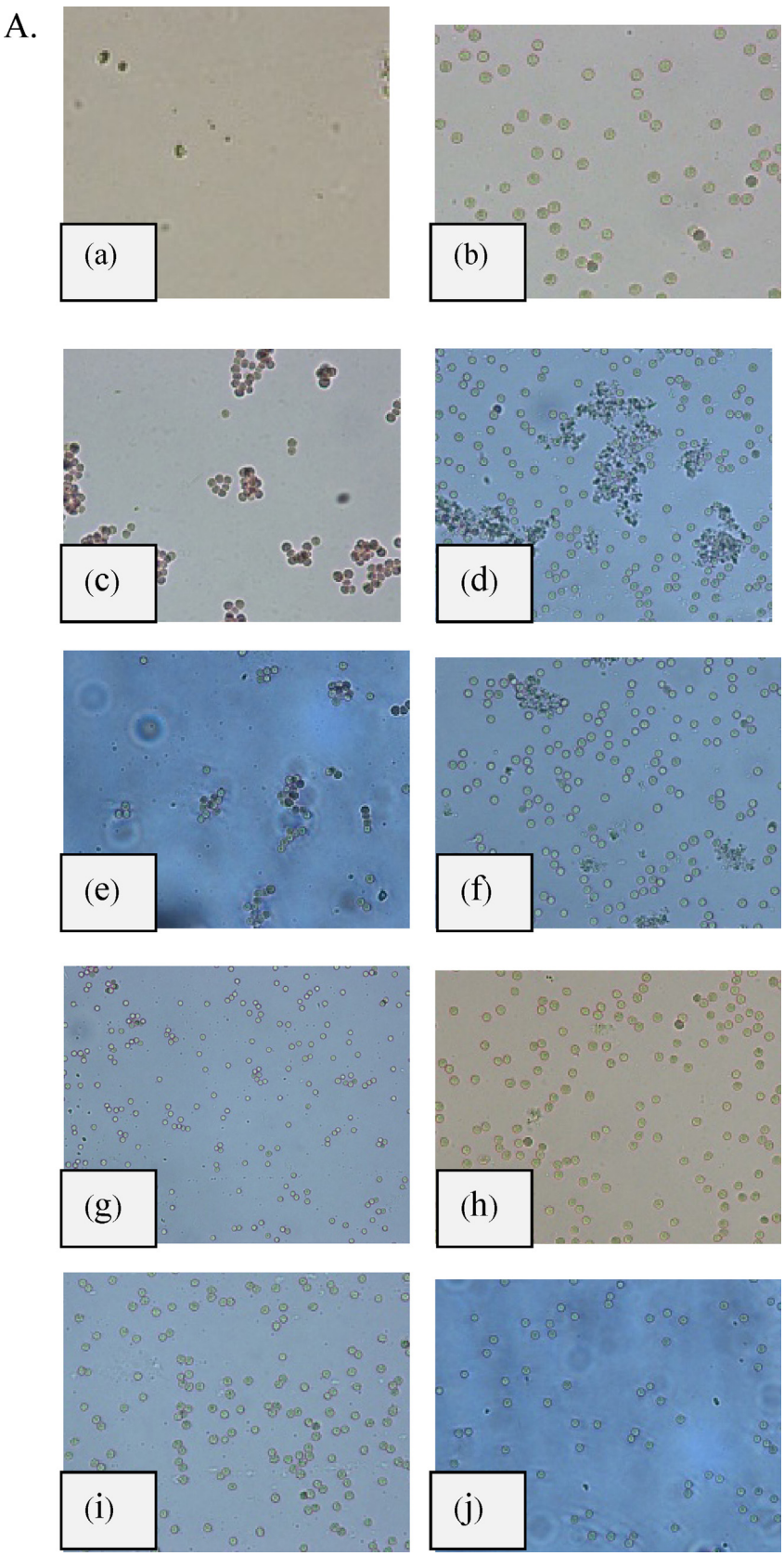

Fig. 3. A. Morphology of the red blood cells of horse after incubation with ZnO NPs, SAGA-ZnO NPs and blank hydrogel at different concent rations a. Positive control (distilled water) b. Untreated erythrocytes (Negative control), c. ZnO NPs at 1.6 μg/μl d. SAGA-ZnO NPs 1.6 μg/μl e. ZnO NPs 0.8 μg/μl, (f) SAGA-ZnO NPs 0.8 μg/μl, g. ZnO NPs 0.2 μg/μl h. SAGA-ZnO NPs 0.2 μg/μl i. ZnO NPs 0.4 μg/μl, j. SAGA-ZnO NPs 0.4 μg/μl. B. Hemolytic assessment of QS-NPs on horse RBCs. Suspension of horse erythrocytes was treated with different concentrations of ZnO NPs, SAGA-ZnO NPs. Percentage of hemolysis caused by ZnO NPs and SAGA-ZnO NPs is shown. Error bars show the standard deviation. *Statistically significant difference compared with controls ($p < 0.05$).

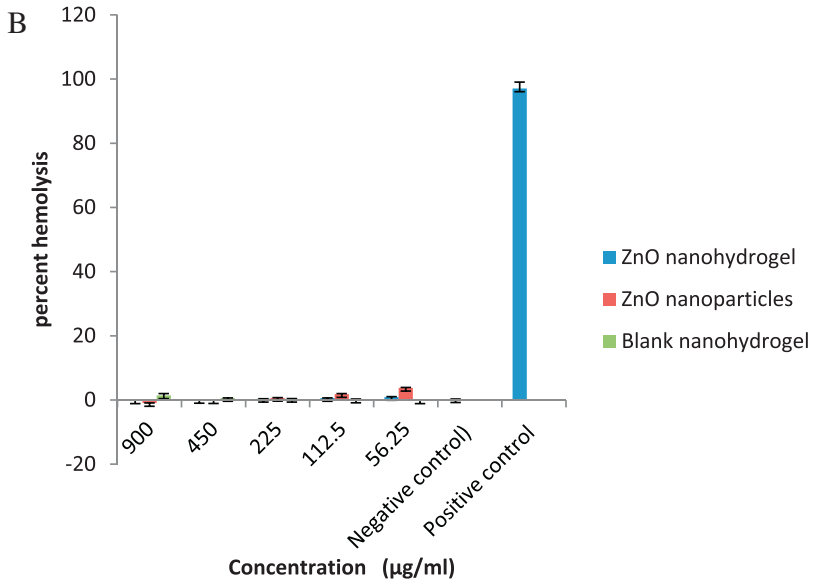

Fig. 3. (*Continued*)

ZnO NPs, SAGA-ZnO NPs and blank hydrogel, aggregation of RBC was observed at higher concentrations (1.6 μg–0.4 μg/μl) of ZnO NPs treated blood sample, but at lower concentrations, no toxic effect was observed. Interestingly, there was an intact RBC population noticed at all the concentration of SAGA-ZnO NPs. Comparative effect of ZnO NPs and SAGA-ZnO NPs over RBC was shown in Fig. 3A. Compatibility testing of the SAGA-ZnO NPs on equine erythrocytes revealed decreased hemolytic rate as compared to ZnO NPs. The hemolysis was significantly lower at different concentrations ($p < 0.5$) as shown in Fig. 3b.

Our study provides a better understanding of the hemolytic and oxidative effects of interaction of ZnO NPs and ZnO NPs released from polymeric hydrogels with the biological system. It can be inferred from this study that normal horse erythrocytes when treated with ZnO NPs in *in vitro* condition undergo oxidative damage, and may be a contributing factor in augmenting the toxicity. We demonstrated implicitly SAGA-ZnO NPs reduced the undesirable effects provoked by ZnO NPs on mammalian cells.

Acknowledgements

The authors thank Indian Council of Agricultural Research, Ministry of Agriculture and farmers welfare, New Delhi, India for providing financial support. The Authors are also grateful to IARI, New Delhi for analysis of samples by TEM.

References

[1] D. Chen, Design: synthesis and properties of highly functional nanostructured photocatalysts, Recent Pat. Nanotechnol. 2 (2008) 183–189.
[2] K. Riehemann, S.W. Schneider, T.A. Luger, B. Godin, M. Ferrari, H. Fuchs, Nanomedicine—challenge and perspectives, Angew. Chem. Int. Ed. Engl. 48 (2009) 872–897.
[3] A. Meghea, Pharmaceuticals and cosmeceuticals based on soft nanotechnology techniques with antioxidative, immunostimulative and other therapeutic activities, Recent Pat. Nanotechnol. 2 (2008) 137–145.
[4] A. Manuja, B. Kumar, R.K. Singh, Nanotechnology developments: opportunities for animal health and production, Nanotechnol. Dev. 2 (1) (2012) e4.
[5] S.J. Klaine, P.J. Alvarez, G.E. Batley, T.F. Fernandes, R.D. Handy, D.Y. Lyon, S. Mahendra, M.J. McLaughlin, J.R. Lead, Nanomaterials in the environment: behavior, fate, bioavailability, and effects, Environ. Toxicol. Chem. 27 (2008) 1825–1851.
[6] P.A. Schulte, D. Trout, R.D. Zumwalde, E. Kuempel, C.L. Geraci, V. Castranova, D.J. Mundt, K.A. Mundt, W.E. Halperin, Options for occupational health surveillance of workers potentially exposed to engineered nanoparticles: state of the science, J. Occup. Environ. Med. 50 (2008) 517–526.
[7] Nanomaterials: toxicity, health and environmental issues, in: C. Kumar (Ed.), Nanotechnologies for the Life Sciences Vol 5, 1st ed., Wiley-VHC, Weinheim, Germany, 2006.
[8] T. Sun, Y. Yan, Y. Zhao, F. Guo, C. Jiang, Copper oxide nanoparticles induce autophagic cell death in A549Cells, PLoS One 7 (8) (2012) 43442.
[9] M. Chopra, M. Bernela, P. Kaur, A. Manuja, B. Kumar, R. Kumar, Alginate/gum acacia bipolymeric nanohydrogels—promising carrier for zinc oxide nanoparticles, Int. J. Biol. Macromol. 72c (2015) 827–833.
[10] D. Xiong, T. Fang, L. Yu, X. Sima, W. Zhu, Effects of nano-scale TiO2, ZnO and their bulk counterparts on zebrafish: acute toxicity, oxidative stress and oxidative damage, Sci. Total Environ. 409 (8) (2011) 1444–1452.
[11] K. Donaldson, V. Stone, Current hypotheses on the mechanisms of toxicity of ultrafine particles, Ann. 1st Super. Sanita 39 (3) (2003) 405–410.
[12] A.A. Shvedova, E.R. Kisin, R. Mercer, A.R. Murray, V.J. Johnson, A.I. Potapovich, Y.Y. Tyurina, O. Gorelik, S. Arepalli, D. Schwegler-Berry, A.F. Hubbs, J. Antoni, D.E. Evans, B.K. Ku, D. Ramsey, A. Maynard, V.E. Kagan, V. Castranova, P. Baron, Unusual inflammatory and fibrogenic pulmonary responses to single-walled carbon nano-tubes in mice, Am. J. Physiol. Lung Cell. Mol. Physiol. 289 (5) (2005) 698–708.
[13] A. Haase, S. Rott, A. Mantion, P. Graf, J. Plendl, A.F. Thunemann, W.P. Meier, A. Taubert, A. Luch, G. Reiser, Effects of silver nanoparticles on primary mixed neural. cell cultures, uptake, oxidative stress and acute calcium responses, Toxicol. Sci. 6 (2) (2012) 457–468.
[14] N. Mei, Y. Zhang, Y. Chen, X. Guo, W. Ding, S.F. Ali, A.S. Biris, P. Rice, M.M. Moore, T. Chen, Silver nanoparticle-induced mutations and oxidative stress in mouse lymphoma cells, Environ. Mol. Mutagen. 53 (6) (2012) 409–419.
[15] W. Maret, C. Jacob, B.L. Vallee, E.H. Fischer, Inhibitory sites in enzymes: zinc removal and reactivation by thionein. a note, Proc. Natl. Acad. Sci. U. S. A. 96 (5) (1999) 1936–1940.
[16] S.J. Lee, K.S. Cho, J.Y. Koh, Oxidative injury triggers autophagy in astrocytes: the role of endogenous zinc, Glia 57 (12) (2009) 1351–1361.
[17] W.Y. Cheng, H. Tong, E.W. Miller, C.J. Chang, J. Remington, R.M. Zucker, P.A. Bromberg, J.M. Samet, T.P. Hofer, An integrated imaging approach to the study of oxidative stress generation by mitochondrial dysfunction in living cells, Environ. Health Perspect. 118 (7) (2010) 902–908.
[18] H.M. Chiang, Q. Xia, X. Zou, C. Wang, S. Wang, B.J. Miller, P.C. Howard, J.J. Yin, F.A. Beland, H. Yu, P.P. Fu, Nanoscale ZnO induces cytotoxicity and DNA damage in human cell lines and rat primary neuronal cells, J. Nanosci. Nanotechnol. 12 (2012) 2126–2135.
[19] B. De Berardis, G. Civitelli, M. Condello, P. Lista, R. Pozzi, G. Arancia, S. Meschini, Exposure to ZnO nanoparticles induces oxidative stress and cytotoxicity in human colon carcinoma cells, Toxicol. Appl. Pharmacol. 246 (2010) 116–127.
[20] I.F. Osman, A. Baumgartner, E. Cemeli, J.N. Fletcher, D. Anderson, Genotoxicity and cytotoxicity of zinc oxide and titanium didoxide in Hep-2 cells, Nanomedicine 5 (8) (2010) 1193–1203.
[21] V. Sharma, D. Anderson, A. Dhawan, Zinc oxide nanoparticles induce oxidative DNA damage and ROS-triggered mitochondria mediated apoptosis in human liver cells (HepG2), Apoptosis 17 (2012) 852–870.
[22] R. Raguvaran, B.K. Manuja, A. Manuja, Zinc oxide nanoparticles: opportunities and challenges in veterinary sciences, Immunome Res. 11 (2) (2015), http://dx.doi.org/10.4172/1745-7580.1000095.

[23] R. Wahab, N.K. Kaushik, A.K. Verma, A. Mishra, I.H. Hwang, Y.B. Yang, H.S. Shin, Y.S. Kim, Fabrication and growth mechanism of ZnO nanostructures and their cytotoxic effect on human brain tumor U87, cervical cancer HeLa, and normal HEK cells, J. Biol. Inorg. Chem. 16 (3) (2011) 431–442.
[24] R. Raguvaran, A. Manuja, S. Singh Chopra, B.K. Manuja, U. Dimri, Zinc oxide nanopartilce induced hemolytic cytotoxicity in horse red blood cells, Int. J. Pharm. Sci. Res. 6 (3) (2015) 1166–1169.
[25] Z. Fan, J.G. Lu, Zinc oxide nanostructures: synthesis and properties, J. Nanosci. Nanotechnol. 5 (2005) 1561–1573.
[26] T. Xia, M. Kovochich, M. Liong, L. Mädler, B. Gilbert, H. Shi, J.I. Yeh, J.I. Zink, A.E. Nel, Comparison of the mechanism of toxicity of zinc oxide and cerium oxide nanoparticles based on dissolution and oxidative stress properties, ACS Nano 2 (2008) 2121–2134.
[27] R. Raguvaran, B.K. Manuja, M. Chopra, R. Thakur, T. Anand, A. Kalia, A. Manuja, Sodium alginate and gum acacia hydrogels of ZnO nanoparticles show wound healing effect on fibroblast cells, Int. J. Biol. Macromol. 96 (2017) 185–191.
[28] A. Manuja, B. Kumar, M. Chopra, A. Bajaj, R. Kumar, N. Dilbaghi, S. Kumar, S. Singh, T. Riyesh, S.C. Yadav, Cytotoxicity and genotoxicity of a trypanocidal drug quinapyramine sulfate loaded-sodium alginate nanoparticles in mammalian cells, Int. J. Biol. Macromol. 88 (2016) 146–155.
[29] S. Singh, M. Chopra, N. Dilbaghi, B.K. Manuja, S. Kumar, R. Kumar, N.S. Rathore, S.C. Yadav, A. Manuja, Synthesis and evaluation of isometamidium-alginate nanoparticles on equine mononuclear and red blood cells, Int. J. Biol. Macromol. 92 (2016) 788–794.
[30] I. Pujalté, I. Passagne, B. Brouillaud, M. Tréguer, E. Durand, C. Ohayon-Courtès, B. L'Azou, Cytotoxicity and oxidative stress induced by different metallic nanoparticles on human kidney cells, Part. Fibre Toxicol. 8 (1) (2011) 10.
[31] G. Gstraunthaler, W. Pfaller, P. Kotanko, Gluthatione depletion and in vitro lipid peroxidation in mercury or maleate induced acute renal failure, Biochem. Pharmacol. 32 (1983) 2969–2972.
[32] S. Syama, S. Reshma, P.J. Sreekanth, H.K. Varma, P.V. Mohanan, Effect of zinc oxide nanoparticles on cellular oxidative stress and antioxidant defense mechanisms in mouse liver, Toxicol. Environ. Chem. 95 (3) (2013) 495–503.
[33] J. Sun, S. Wang, D. Zhao, F.H. Hun, L. Weng, H. Liu, Cytotoxicity, permeability and inflammation of metal oxide nanoparticles in human cardiac microvascularendothelial cells, Cell. Biol. Toxicol. 27 (5) (2011) 333–342.
[34] V. Valdiglesias, C. Costa, G. Kiliç, S. Costa, E. Pásaro, B. Laffon, J. Paulo Teixeira, Neuronal cytotoxicity and genotoxicity induced by zinc oxide nanoparticles, Environ. Int. 55 (2013) 92–100.
[35] M. Simundic, B. Drasler, V. Sustar, J. Zupanc, R. Stukelj, D. Makovec, D. Erdogmus, H. Hagerstrand, D. Drobne, V. Kralj-lglic, Effect of engineered TiO2 and ZnO nanoparticles on erythrocytes, platelet-rich plasma and giant unilamelar phospholipid vesicles, BMC Vet. Res. 7 (9) (2013) 1–13.